QIRT'2022

10.21611/qirt.2022.1023

16th Quantitative InfraRed Thermography Conference

Experimental verification of non-Fourier heat transfer in a multilayer skin tissue structure by IR temperature measurement

by M. Strąkowska*, G. De Mey**, B. Więcek*

* *Institute of Electronics, Lodz University of Technology, Poland*
** *Department of Electronics and information Systems, Ghent University, Belgium*

Abstract

The paper presents experimental verification of the Dual-Phase-Lag (DPL) heat transfer model of a skin tissue. The simulation for Fourier- Kirchhoff and the DPL thermal models was performed for the same set of the parameters. These models were solved analytically in frequency domain using the Laplace transform. The non-Fourier heat transfer should be considered in a tissue as it is a multilayer structure where the perfusion plays an important role in heat transfer. The DPL effect can be visualize in the high frequency range of the Nyquist plot of thermal impedance. Because of that the experiment for living skin tissue was performed using a fast cooled single-detector IR head with the high sampling rate. Based on the obtained data, the DPL model parameters were identified. It confirmed that such model fits well to measurements results and the values of the parameters are agreed with the literature.

1. Introduction

Thermal modelling of the skin is the field of interest for many researchers. Knowing both thermal parameters of the skin and its reaction to thermal excitation, it is useful to describe pathologies of the skin tissue like tumors, psoriasis and inflammations including pre-cancerous lesions and severe cancers. Skin is a complex structure with three or more layers. There are different approaches to thermal modelling such structures [1],[2],[3],[4],[5],[6]. The most common is the Fourier-Kirchhoff (F-K) heat transfer model, but it does not take into account heat transfer by blood flow in both large and capillary vessels. Many models are the modification of the Fourier-Kirchhoff one, e.g. the Pennes [1] model which assumes the presence of perfusion. The Dual-Phase-Lag (DPL) model assumes that there are additional delays for heat flux and temperature [7],[8],[9],[10],[11],[12],[13],[14],[15],[16],[17],[18],[19],[20],[21],[22]. This effect is described by 2 thermal time constants: the relaxation time constant τ_q which indicates the time lag caused by the finite propagation time of heat flux in a tissue and another thermalization time constant τ_T - equation eq. (1). In the literature there are many simulation results of DPL models, both for solids and bio-structures.

$$q(x, t + \tau_q) = -k\nabla T(x, t + \tau_T) \tag{1}$$

Most of them present the numerical solutions. For tissues, the values of parameters especially for DPL model are very different in many papers [16], [17], [18], [19], [20], [21]. The thermalization time varies from few milliseconds to few tens of seconds [14],[15], [16], [17]. The similar variation of the relaxation time constant for tissues are reported in literature. In this paper the experimental results of skin tissue DPL thermal modelling are presented.

2. Simulation results

Parameters of the DPL thermal model can be estimated by solving the model in the frequency domain. Moreover the redefinition of thermal conductivity as a complex number (eq. (2)) has been already presented [22]. The Dual Phase Lag model assumes that the heat is transferred not only due to the temperature gradient. Thermal energy can be transferred if either temperature or heat flux are varying in time. In consequence, two thermal time constants are introduced displaying both an additional relaxation of heat τ_q and a lag of temperature τ_T [22]. The Laplace transform allows to redefine thermal conductivity that can be implemented in Fourier-Kirchhoff energy equation including perfusion [22].

$$\widetilde{k} = k\frac{1 + s\tau_T}{1 + s\tau_q} \tag{2}$$

In frequency domain the model has analytical solution for infinite, semi-infinite and a single slab geometry. For multilayer structures it is possible to formulate the set of linear equations using the interface and boundary conditions [23]. The simulation of F-K and DPL model was performed for 4-layer structure with the parameters listed in table 1.

For F-K model the values of τ_q and τ_T are equal to 0. The simulation was performed for the assumption that the heat source is at one side of the structure. Heat flux $q = 100\ W/m^2$, surface $S = 0.01\ m^2$ and heat transfer coefficient on both sides $h = 5\ W/m^2K$ were selected. This conditions are adequate to the performed IR experiment where the skin is cool down and temperature evolution in time is registered on the skin surface after removing the heat source. Finally, the thermal impedance obtained from the models is presented as the Nyquist plots. Comparison of the plots for F-K and DPL thermal

Table 1. *Model's parameters*

Layer	$k, (W/mK)$	$cv, (J/m^3K)$	$d, (m)$	$\tau_q, (s)$	$\tau_T, (s)$
1	1.5	3e6	0.5e-3	0	0
2	2	4e6	2e-3	2	10
3	3	4e6	5e-3	2	10
4	4	4e6	10e-3	0	0

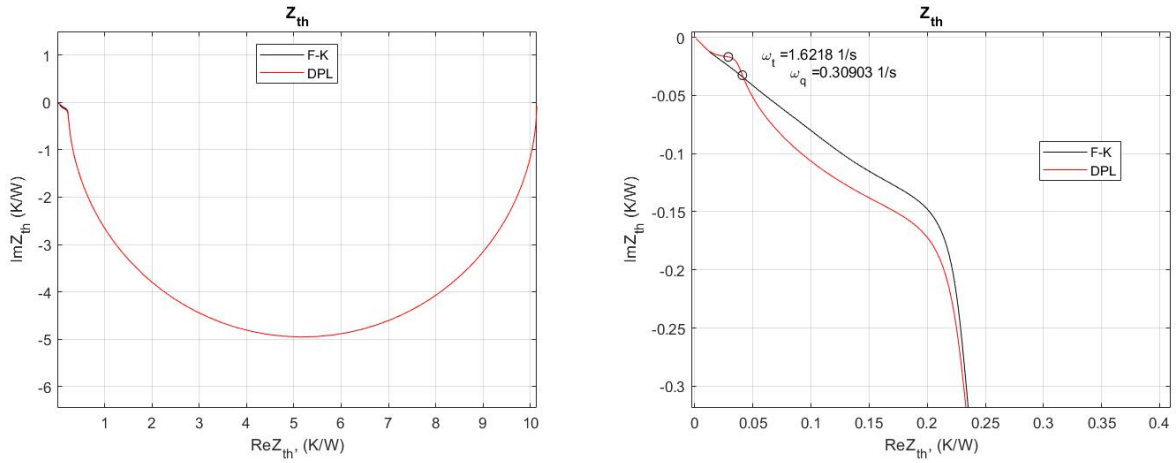

(a) (b)

Fig. 1. *Nyquist plots for F-K and DPL model. (a) - for pulsation in range from* $\omega = 1u$ *to* $1000\ rad/s$ *(b) - for high frequencies -* ω_q *corresponds to* τ_q*,* ω_t *-* τ_t

models is presented in figure 1(a). They show that non-Fourier effect is visible in high frequencies as a non-straight line - figure 1(b). The difference is caused by presence of the relaxation and thermalization time constants.

In order to verify the correctness of the proposed approach and to visualize the difference in time domain, the identification of thermal time constants was performed [24]. This is done by using the transfer function estimation (TFEST) implemented in the Matlab environment with the assumption of 6-pole thermal impedance eq. (3).

$$Z(j\omega) = \sum_{i=1}^{6} \frac{R_i}{1 + j\omega\tau_i} \tag{3}$$

The approximated values of time constants for each poles obtained from the model are in the table 2. This procedure allows to find temperature response vs. time for power excitation in the form of the Heaviside step function eq. (4).

$$T(t) = P_0 \sum_{i=1}^{6} R_i (1 - e^{-\frac{t}{\tau_i}}) \tag{4}$$

The plot of temperature in time is shown in figure 2(a). Additionally, figure 2(b) presents zoomed region where the delay of temperature response can be noticed for the DPL model in comparison to the F-K model.

Table 2. *Models parameters*

i	F-K - $R_i, (K/W)$	F-K - $\tau_i, (s)$	DPL - $R_i, (K/W)$	DPL - $\tau_i, (s)$
1	0.005	0.005	0.004	0.004
2	0.014	0.121	0.0130	0.104
3	0.026	0.906	0.019	0.492
4	0.053	5.795	0.050	11.981
5	0.131	33.315	0.143	38.232
6	9.906	6986.852	9.906	6986.923

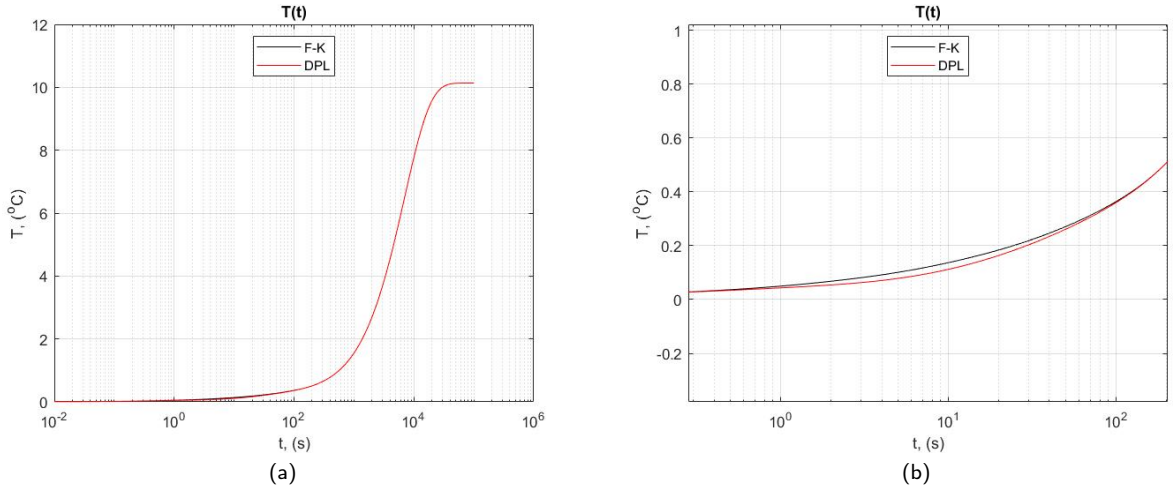

Fig. 2. *(a) - Evaluation of temperature in time for F-K and DPL models (b) - Delay seen for DPL model.*

3. Measurement results

The experiment was conducted using the infrared thermography for registration of temperature change after cold provocation of a skin tissue [25], [26], [27]. The part of the palm is cooled down by a few degrees by a Peltier cooler device.

Fig. 3. *Measurement stand with IR cooled single-detector head*

In the experiment, the photon, cooled, single-detector IR head with the extended sampling rate up to 1 MHz was used [28] as shown in figure 3. Based on the simulation results one can assume that the non-Fourier heat transfer effect can be seen for very short time (sometimes of the order of microseconds or lower), and standard thermal camera might be insufficient for such an experiment. Due to the reported in the literature values of the DPL model parameters, it possible to conclude that thermal time constants for biomedical objects are not at the level of microseconds [15], [16], but it was not confirmed experimentally yet.

The measurement of temperature (in isothermal units) in time from the region of about $1mm^2$ presented in figure 4(a) allows to register temperature with the high frequency rate but it generates a high-level noise, not only caused by sensitivity of the sensor but also by the movement of the measured object. In this research the movement correction is not implemented yet, but using the Kalman filter allows to reach quite smooth curve with reduced noise.

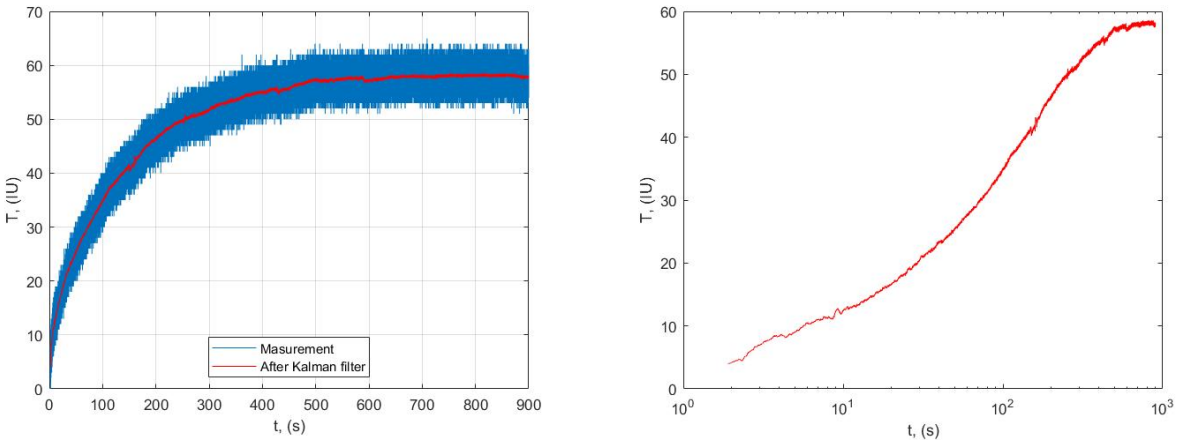

Fig. 4. *(a) - Measurement of temperature in time with and without the Kalman filter (b) - Approximated temperature in time in log scale.*

4. Conclusion

In this paper we presented a simple experiment that confirmed the non-Fourier heat transfer in a multilayer skin tissue structure. The experimental results were compared with simulations performed by the semi-analytical 1D model in frequency domain. A fast single-detector IR head for temperature measurement was used. The results obtained confirm the redefined formula of thermal conductivity for a material where DPL effect occurs.

References

[1] H. Pennes. Analysis of tissue and arterial blood temperature in resting human forearm. *Journal Appl. Physiol.*, 1(2):93–122, 1948.

[2] H. Klinger. Heat transfer in perfused biological tissue - i: General theory. *Bulletin of Mathematical Biology*, 36:403–415, 1974.

[3] K. A. Seffen E. Y. K. Ng F. Xu, T. J. Lu. Mathematical modeling of skin bioheat transfer. *Applied Mechanics Reviews*, 62(5), 2009.

[4] Vincent Costalat Franck Jourdan Domoina Ratovoson, Vincent Huon. Combined model of human skin - heat transfer in the vein and tissue: experimental and numerical study. *Quantitative InfraRed Thermography Journal*, 8(2):165–186, 2011.

[5] K. R. Holmes M. M. Chen. Microvascular contributions in tissue heat transfer. *Annals of The New York Academy of Sciences*, 335(1):137–150, 1980.

[6] F.J. Huygen F.C. van der Helm S. Niehof A.C. Schouten Y. Wu, M.D Nieuwenhoff. Characterizing human skin blood flow regulation in response to different local skin temperature perturbations. *Microvascular Research*, 111(1):96–102, 2017.

[7] D.Y. Tzou. Macro-to microscale heat transfer: The lagging behavior. Second Edition. Wiley, 2014.

[8] Yan-Nan Wang Kuo-Chi Liu, Po-Jen Cheng. Analysis of non-fourier thermal behavior for multi-layer skin model. *Thermal Science*, 15(1):61–67, 2011.

[9] Seung Gyu Park Soon-Ho Choi Jae Hyuk Choi, Seok-Hun Yoon. Analytical solution of the cattaneo vernotte equation (non-fourier heat conduction). *Journal of the Korean Society of Marine Engineering*, 40(5):389–396, 2016.

[10] Y. Zhang. Generalized dual-phase lag bioheat equations based on nonequilibrium heat transfer in living biological tissues. *International Journal of Heat and Mass Transfer*, 52(5):4829–4834, 2009.

[11] M. Paruch B. Mochnacki. Cattaneo-vernotte equation. identification of relaxation time using evolutionary algorithms. *Journal of Applied Mathematics and Computational Mechanics*, 12(4):97–102, 2013.

[12] J. Dziatkiewicz E. Majchrzak, Ł. Turchan. Modeling of skin tissue heating using the generalized dual phase-lag equation. *Journal of Applied Mathematics and Computational Mechanics*, 67(6):417–437, 2015.

[13] A. Samson P. Zając M. Zubert, T. Raszkowski. Methodology of determining the applicability range of the dpl model to heat transfer in modern integrated circuits comprised of finfets. *Microelectronics Reliability*, 91(1):139–153, 2018.

[14] Y. Zhang. Generalized dual-phase lag bioheat equations based on nonequilibrium heat transfer in living biological tissues. *International Journal of Heat and Mass Transfer*, 52(21-22):4829–4834, 2009.

[15] V.K. Katiyar S. Telles A. Kumar, S. Kumar. Dual phase lag bio-heat transfer during cryosurgery of lung cancer: Comparison of three heat transfer models. *Journal of Thermal Biology*, 69:228–237, 2017.

[16] A.K. Vashishth R. Kumar and S. Ghangas. Phase-lag effects in skin tissue during transient heating. *International Journal of Applied Mechanics and Engineering*, 24(3):603–623, 2019.

[17] S. Kumar S. Singh. Numerical study on triple layer skin tissue freezing using dual phase lag bio-heat model. *International Journal of Thermal Sciences*, 86:12–20, 2014.

[18] Jing Liu Zhong-Shan Deng. Non-fourier heat conduction effect on prediction of temperature transients and thermal stress in skin cryopreservation. *Journal of Thermal Stresses*, 26(8):779–798, 2003.

[19] Qing-Hua Qin Xiaogeng Tian Xiaoya Li, Pengfei Luo. The phase change thermoelastic analysis of biological tissue with variable thermal properties during cryosurgery. *Journal of Thermal Stresses*, 43(8):998–1016, 2020.

[20] T. B. Pavan Kumar Ramgopal Uppaluri Ranjan Das, Subhash C. Mishra. An inverse analysis for parameter estimation applied to a non-fourier conduction- radiation problem. *Heat Transfer Engineering*, 32(6):455–466, 2011.

[21] Anil Stephen Subhash C. Mishra. Combined mode conduction and radiation heat transfer in a spherical geometry with non-fourier effect. *International Journal of Heat and Mass Transfer*, 54(13-14):2975–2989, 2011.

[22] B. Wiecek M. Strakowska, G. De Mey. Comparison of the fourier-kirchhoff, pennes and dpl thermal models of a single layer tissue. 09 2020.

[23] B. Więcek M. Strąkowska, G. De Mey. Identification of the thermal constants of the dpl heat transfer model of a single layer porous material. *Pomiary Automatyka Robotyka*, 25(2):41–46, 2021.

[24] G. De Mey V. Chatziathanasiou B. Więcek M. Strakowska, P. Chatzipanagiotou. Multilayer thermal object identification in frequency domain using ir thermography and vector fitting. *International Journal of Circuit Theory and Applications*, 48(9):1523–1533, 2020.

[25] L. Pfaffmann U. Reinhold T. M. Buzug, S. Schumann and J. Ruhlmann. Functional infrared imaging for skin-cancer screening. pages 2766–9, 01 2006.

[26] J.Ruminski M. Hryciuk A. Nowakowski, M.Kaczmarek. Postępy termografii - aplikacje medyczne. Wydawnictwo Gdańskie, 2001.

[27] A. Renkielska J. Grudziński W. Stojek M. Kaczmarek, A. Nowakowski. Investigation of skin burns basing on active thermography. volume 3, pages 2882–2885, 2001.

[28] M. Kopec and B. Wiecek. Low-cost ir system for thermal characterization of electronic devices. *Measurement Automation Monitoring*, 64(4):103–107, 2018.